SUPER ELEMENT MODEL DEVELOPMENT AND ANALYSIS ON THE MARK I TORUS STRUCTURE

L.-C. HUA

Bechtel Power Corporation, P.O. Box 3965, San Francisco, California 94119, U.S.A.

The Mark I BWR pressure suppression system consists of a toroidal shell suppression chamber and a vent pipe system. The suppression system is presently under structural performance evaluations for the static and dynamic loads resulting from the Loss-of-Coolant Accident (LOCA) and Safety Relief Valve (SRV) discharge. This evaluation necessitates the accurate determination of the system response and structural stresses under all SRV and LOCA related loading conditions.

The purpose of this report is to describe the development of a finite element model and analysis procedures, using the "super element" capability of the NASTRAN computer program, for the static and dynamic analysis of the Mark I torus structure; and to present the results of the analyses performed in this work for a specific Mark I torus.

One important consideration in the torus finite element model development was the model be sufficiently refined such that it could be used for analyzing all necessary loading conditions, and could yield accurate enough stress information for a direct code evaluation. Thus, a very large finite element model is necessary. The model reported here consists of 5998 nodes and 6512 elements with 35988 total system degrees-of-freedom to represent one-half of torus structure. In comparison with a number of model developed to date for the torus structural evaluation, this model is the most comprehensive one.

Two static and three dynamic analyses were performed based on this model. The first static analysis considered the combined loading of the LOCA pressurization load and the dead load including the hydrostatic pressure load. The second static analysis considered the peak pressure distribution of the peak chugging load for the purpose of determining the dynamic amplification factors of the structure due to the dynamic chugging loads. The dynamic analyses performed were for the 8 and 20 Hz dynamic chugging loads. Two types of water mass distribution methods were considered; the radial distribution and the hydrostatic distribution. This was done for the purpose of studying the primary modes associated with the different types of water mass distribution.

The results of the analyses performed show that:

- The stresses in the structure are highly sensitive to the excitation frequencies. In order to assure that every component of the structure is excited to its maximum level within the frequency range, a complete evaluation should consider many different excitation frequencies.

- There are significant coupling effects between torus segments. These effects can be properly studied only with the type of model reported herein.

- The frequency content and mode shapes are significantly affected by the water mass distribution methods. The radial mass distribution induces oval shapes modes of the torus while the hydrostatic mass distribution induces bounce modes of the whole structure.

1.0 INTRODUCTION

The purpose of this report is to describe the development of a finite element model and analysis procedures, using the "super element" capability of the NASTRAN computer program. for the static and dynamic analysis of the Mark I torus structure; and to present the results of the analyses performed in this work for a specific Mark I torus.

One important consideration in the torus finite element model development was the model be sufficiently refined such that it could be used for analyzing all neccessary loading conditions, and could yield accurate enough stress information for a direct code evaluation. Thus, the development of the torus model configuration and finite element mesh sizes were largely dictated by this consideration.

Two static and three dynamic analyses were performed based on this model. The first static analysis considered the combined loading of the LOCA pressurization load and the dead load including the hydrostatic pressure load. The second static analysis considered the peak pressure distribution of the peak chugging load for the purpose of determining the dynamic amplification factors of the structure due to the dynamic chugging loads. The dynamic analyses performed were for the 8 and 20 Hz dynamic chugging loads. Two types of water mass distribution methods were considered; the radial distribution and the hydrostatic distribution. This was done for the purpose of studying the primary modes associated with the different types of water mass distribution.

The analyses performed are intended not only to demonstrate the effectiveness and efficiency of using the super element approach for the anlysis of torus structures, but also to generate detailed response results which can be used for code evaluations for the load cases considered. Representative results of displacements and reactions obtained in these analyses are presented along with the result discussions relating to the torus response to the dynamic chugging load.

2.0 DESCRIPTION OF THE TORUS STRUCTURE

The general configuration of the Mark I torus suppression chamber is the same for all Mark I plants. However the structural dimensions and design details differ among plants. In general, the torus is made up of an assemblage of mitered, steel cylindrical shell adjacent to each miter joint. The entire torus is supported on steel columns, arranged in pairs attached to each ring stiffener.

The torus shell is about half-filled with water acting as a suppression pool. The ring header and downcomers of the vent pipe system are housed inside the torus. The ring header and downcomers are supported partially by steel columns attached to the bottom of the torus shell, and partially by the vent pipes which connect the ring header to the reactor drywell.

Figure 1 shows the configuration of a specific Mark I torus. This particular torus was used for the detailed finite element model development and response analyses. The shell of this torus was fabricated from two plate thicknesses, 0.604" for the upper half and 0.675" for the lower half of the shell. The torus cylinder has an inner radius of 15'-6" with a minimum water depth of 14'-6", as shown in Figure 2.

3.0 LOADING CONDITIONS

The loading conditions to be considered for the torus structural evaluation are as described in the following:

a) Dead Load (D)
b) Seismic Loads (E)
c) Torus Pressurization Load (P_a)
d) Condensation Oscillation Load (CO)
e) Chugging Load (CH)
f) Pool Swell Load (PS)
g) Safety Relief Valve Discharge Load (SRV)

4.0 SUPER ELEMENT FORMULATION

For static analysis, the formulation of super element involves the static condensation process identical to the substructuring formulation. For dynamic analysis, additional operations based on the Guyan reduction technique are required.

The static equilibrium equations of a super element can be written as:

$$\begin{bmatrix} K_{aa} & K_{ao} \\ K^T_{ao} & K_{oo} \end{bmatrix} \begin{Bmatrix} U_a \\ U_o \end{Bmatrix} = \begin{Bmatrix} P_a \\ P_o \end{Bmatrix} \qquad (1)$$

where:

U_a = the displacement vector associated with the exterior degrees-of-freedom (DOFs) which include the boundary DOFs and those interior DOFs designated to be the dynamic DOFs for dynamic analysis.
U_o = the displacement vector associated with the interior DOFs which are the total DOFs excluding those in U_a.
K_{aa} = the stiffness matrix assoicated with the displacement vector U_a.
K_{oo} = the stiffness matix associated with the displacement vector U_o.
K_{ao} = the coupling stiffness matrix assoicated with the displacement vectors U_a and U_o.
P_a = the loads applied on the U_a exterior DOFs.
P_o = the loads applied on the U_o interior DOFs.

By the standard matrix operation, the displacements of the interior DOFs can be expressed in terms of those of the exterior DOFs in the form:

$$\{U_o\} = \{G_o\} \quad \{U_a\} + \{U_o^o\} \qquad (2)$$

where

$$[G_o] = -[K_{oo}]^{-1} [K_{ao}]^T \qquad (3)$$

$$\{U_o^o\} = [K_{oo}]^{-1} \{P_o\} \qquad (4)$$

Substituting Eq. (2) into Eq. (1) and neglecting the term $\{U_o^o\}$ which is usually small, Eq. (1) can be reduced to:

$$[\bar{K}_{aa}]\{U_a\} = \{\bar{P}_a\} \qquad (5)$$

where,

$$[\bar{K}_{aa}] = [K_{aa}] + [K_{ao}] [G_o] \qquad (6)$$

$$\{\bar{P}_a\} = \{P_a\} + [G_o]^T\{P_o\} \qquad (7)$$

Equation (5) represents the reduced equilibrium equations of a super element.

In static analysis, the equilibrium equations of the entire structure can be obtained by assembling the equilibrium equations of all super elements in the structure. The resulting equations subjected to the prescribed displacement boundary condition and applied loads can be solved for the displacement solution $\{U_a\}$ of each super element. The solution for $\{U_o\}$ can then be obtained by substituting $\{U_a\}$ into Eq. (2).

For dynamic analysis, the equations of motion contain the mass and damping terms in addition to the stiffness term. Utilizing the Guyan reduction technique, the mass and damping terms of a super element can be consistently reduced in a manner similar to the stiffness matrix using the same transformation matrix $[G_o]$. The mass matrix so reduced can be expressed as:

$$[\bar{M}_{aa}] = [M_{aa} + M_{ao}G_o + G_o^T M_{ao}^T + G_o^T M_{oo} G_o] \qquad (8)$$

and the reduced damping matrix is:

$$[\bar{C}_{aa}] = [C_{aa} + C_{ao}G_o + G_o^T C_{ao}^T + G_o^T C_{oo} G_o] \quad (9)$$

The reduced equations of motion for a super element can be written as:

$$[\bar{M}_{aa}] \{\ddot{U}_a\} + [\bar{C}_{aa}] \{\dot{U}_a\} + [\bar{K}_{aa}] \{U_a\} = \{\bar{P}_a\} \quad (10)$$

where $\{\ddot{U}_a\}$ and $\{\dot{U}_a\}$ are the acceleration and velocity vector respectively, corresponding to the displacment vector $\{U_a\}$. The equations of motion for the entire system can be obtained by assembling Eq. (10) for all super elements in the structure and by prescribing the system boundary conditions. The resulting equations of motion as obtained include all the system dynamic DOFs and the boundary DOFs of the super elements which are not necessarily all dynamic DOFs. The remaining static DOFs can be eliminated again by the second application of the Guyan reduction technique. The second Guyan reduction reduces the equations of motion to those only associated with the system dynamic DOFs. This final system of equations of motion can be solved by the standard time history response analysis procedure. Then the responses of the static DOFs can be obtained by systematic back-substitutions twice corresponding to the twice Guyan reduction processes.

5.0 FINITE ELEMENT MODEL

A 180° finite element model for half of the torus structure shown in Figures 5(A) through 5(D) was developed based on the super element formulation. The model consists of eight super elements. Each super element represents a typical 22.5° torus segment from the midspan of the torus between column lines to the adjacent midspan.

The basic finite element used in the super element model was the NASTRAN QUAD4 shell element. The element is an isoparametric, quadrilateral thin shell element with transverse shear energy corrections. It has good convergence characteristics, thus enabling good results with relatively coarse mesh. Besides the QUAD4 elements, the NASTRAN beam, linkage (truss), and spring elements were also used in the super element model.

The finite element mesh for a basic 22.5° torus segment consists of 46 divisions in the torus cross-section and 12 divisions along the torus axis between the midspans. The mesh density near the miter plane and column supports were increased three times for anticipated higher stress gradient in these regions. The ring girder web was modeled by two layers of shell elements, thus permitting direct outputs of web stresses. The ring girder flange and supporting columns were modeled by beam elements. The column-to-ring girder junction was modeled by a combination of triangular shell elements and beam elements. The stiffnesses of the vent system and downcomer support columns were modeled by generalized spring elements fixed at one end to simulate the fixity condition at the drywell. The resulting finite element model of the 22.5° torus segment is shown in Figures 5(A) and 5(B). It contains 790 nodes with 4740 total DOFs, and a total of 864 elements including 744 shell elements, 64 beam elements, 2 linkage elements, and 4 spring elements.

For dynamic analysis, each super element was assigned 75 mass points. Fifteen mass points were evenly distributed along a nodal ring in the torus cross-section. Five rings of mass points were located at the midspan, quater spans, and the miter joint of the torus segment. Each mass point in the model had up to three translational dynamic DOFs.

The hydrodynamic masses due to contained water were included in the radial directions of the shell. These masses were computed on the basis of tributary hydrostatic pressure and pie shaped cross-section to each respective mass point. Damping in the structure was modeled using the stiffness proportional damping.

The 180° half torus model as shown in Figure 5(C) was obtained by assembling eight super elements described above. The final model consists of 5998 nodes and 6512 elements with 35,988 total nodal DOFs. For static analysis, the entire system of the half torus model was reduced to 384 nodes totaling 2304 static equilibrium equations.

In dynamic analysis, the first Guyan reduction reduced the system to 774 nodes with

4644 system DOFs. The second Guyan reduction further reduced the system down to 700 equations of motion corresponding to 700 system dynamic DOFs.

6.0 ANALYSIS PROCEDURES

The step-by-step procedures for performing the analysis of the torus using the NASTRAN program are summarized in the following:

1) Generate load, mass, damping and stiffness matrices for the basic super element.
2) Reduce super element matrices to those associated with the exterior DOFs.
3) Assemble the reduced matrices of all super elements for the half torus model. The structure represented by these matrices is called the "residual structure".

In the static analysis, steps 4) through 6) were performed:

4) Decompose the stiffness matrix of residual structure and back substitute with reduced load matrix to obtain the displacements of the residual structure.
5) Substitute the displacements of residual structure in the reduced super element matrices to calculate the remaining displacement of the super elements.
6) Compute element forces and stresses from super element displacements.

For dynamic analysis, steps 7) through 12) were executed:

7) Reduce the residual structural matrices to those associated with the system dynamic DOFs only.
8) Decompose the doubly reduced matrices.
9) Integrate the resulting equations of motion to solve for the time history displacements of the dynamic DOFs.
10) Expand the time history displacements of the dynamic DOFs to the time history displacements of residual structure.
11) Substitute the time history displacements of residual structure in the reduced super element matrices to calculate the remaining time history displacements of super element.
12) Compute the time history element forces and stresses from the time history displacements of super element.

7.0 RESULTS

The analysis work performed in the study consists of two static analyses for the combined dead and torus pressurization loads ($D + P_a$) and three dynamic analyses for the 8 and 20 Hz dynamic chugging loads (CH). The 20 Hz chugging load dynamic analysis was considered to be the reference load case. The 8 Hz chugging load analysis was performed to assess the dynamic response characteristics of the torus as the chugging load frequency varies. A separate static analysis of the torus subjected to the peak chugging load was also performed to determine the dynamic amplification factors of the structure due to the dynamic chugging load.

Representative results obtained from these analyses are presented to illustrate the general behavior of the structure under the loading conditions considered.

Table 1 presents the column reactions obtained from the static analysis for the peak chugging load. The magnitude of the column reactions conform well with the shape of load distribution along the torus axis.

Table 2 shows the maximum column reactions of the torus subjected to the 8 and 20 Hz dynamic chugging load. Comparing the results in this table and Table 1 the dynamic amplification factors of the column reactions ranges from 50% to 190% of static reactions. This range of values clearly demonstrated the influence of excitation frequency and mass distribution on the responses of the structure.

Figure 3 and 4 shows some typical column reaction and shell displacement time histories for the chugging load cases. It can be seen from these figures that the column reactions have a predominant natural frequency of about 7 Hz and 14 Hz, depending on the assumption of mass distribution. The response of these modes dominate the column reaction time histories for the 8 Hz loading, whereas, for the 20 Hz loading, the response of this mode is superimposed by an out-of-phase torus twisting mode which caused the maximum inner column reactions to be slightly larger than those of the outer columns.

8.0 SUMMARY AND CONCLUSIONS

A finite element model and analysis procedures for the static and dynamic analysis of the torus using the latest features, the super element formulation and multiple Guyan reductions, of the NASTRAN program have been developed. In the present day application of finite element analysis method, this is an advanced application of the method.

Because of the large number of elements and highly refined finite element mesh used in this model, accurate prediction of local responses as well as gross responses can be accomplished. By the use of super elements, the data preparation associated with the model development can be fully automated, thus not only reducing the total effort of model development, but also minimizing the errors in the data preparation. By means of double Guyan reduction, the large finite element model of the torus can be reduced to a much smaller dynamic model. The analysis of this model requires only moderate amounts of computer resources and can be carried out efficiently and economically. Further refinements, if required, are computationally feasible.

The results of the analyses performed show that:

- The responses of the structure are highly sensitive to the excitation frequencies. In order to assure that every component of the structure is excited to its maximum level within the frequency range, a complete evaluation should consider many different excitation frequencies.

- There are significant coupling effects between torus segments. These effects can be properly studied only with the type of model reported herein.

- The frequency content and mode shapes are significantly affected by the water mass distribution methods. The radial mass distribution induces oval shaped modes of the torus while the hydrostatic mass distribution induces bounce modes of the whole structure.

Table 1 Column Reactions Under Static Peak Chugging Load

Column Line	Vertical Reactions in kips	
	Inner Column	Outer Column
1	146.7	200.8
2	127.1	162.6
3	115.7	149.2
4	109.7	143.8
5	106.9	141.1
6	103.8	134.6
7	101.4	129.3
8	102.2	133.4

Table 2 Maximum Column Reaction Under Dynamic Chugging Loads, Outer Column

Column Line	8 Hz Chugging Load		20 Hz Chugging Load			
	Maximum Reaction (kips)	Time Of Maximum (sec)	Maximum Reaction (kips)	Time Of Maximum (sec)	Maximum Reaction* (kips)	Time Of Maximum (sec)
1	-393.7	0.124	-110.0	0.076	-261.0	0.052
2	-320.4	0.124	-87.7	0.076	-221.0	0.052
3	-297.7	0.124	-79.7	0.076	-181.0	0.052
4	-292.4	0.124	-76.6	0.076	-161.0	0.052
5	-290.4	0.124	-76.4	0.076	-152.0	0.052
6	-288.6	0.124	-76.4	0.076	-151.0	0.052
7	-286.9	0.124	-76.8	0.076	-152.0	0.052
8	-285.9	0.124	-77.0	0.076	-153.0	0.052

*Pie-shape mass distribution

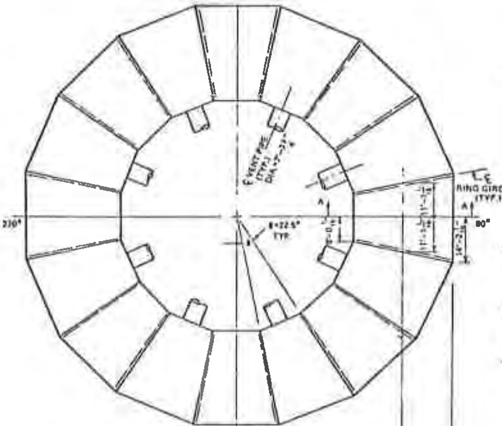

FIGURE 1
TORUS PLAN

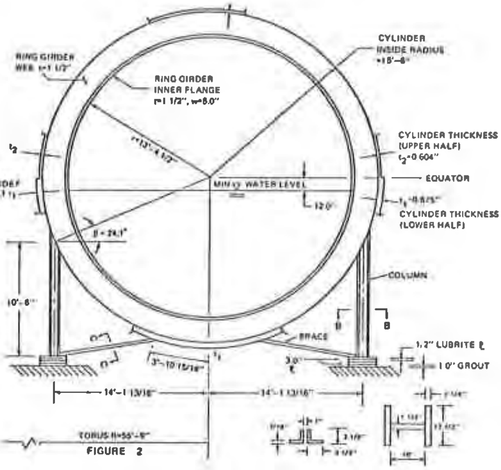

FIGURE 2
TORUS SECTIONS AND DETAILS

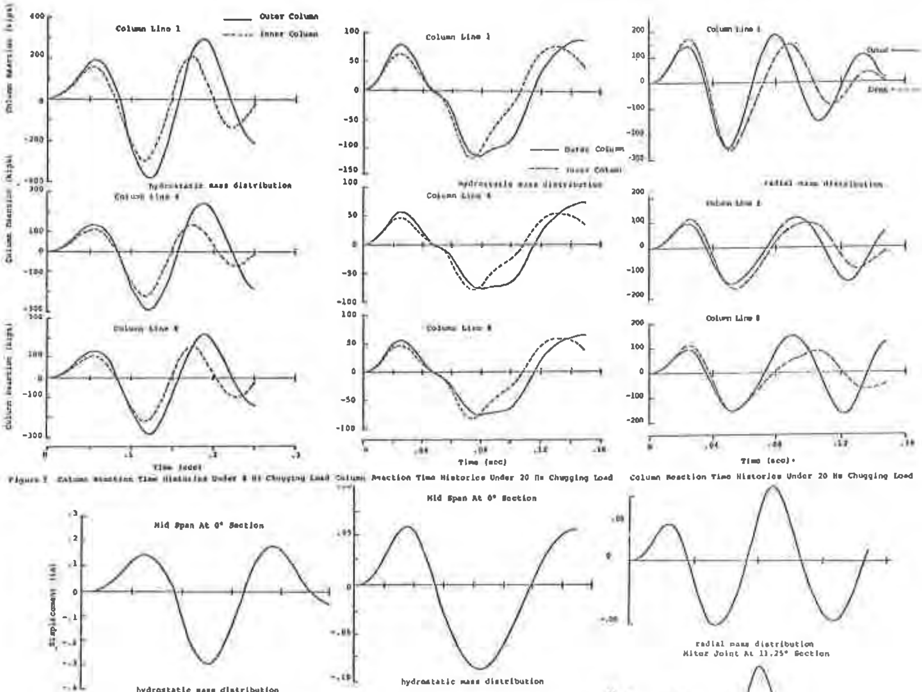

Figure 3 Column Reaction Time Histories Under 8 Hz Chugging Load

Column Reaction Time Histories Under 20 Hz Chugging Load

Column Reaction Time Histories Under 20 Hz Chugging Load

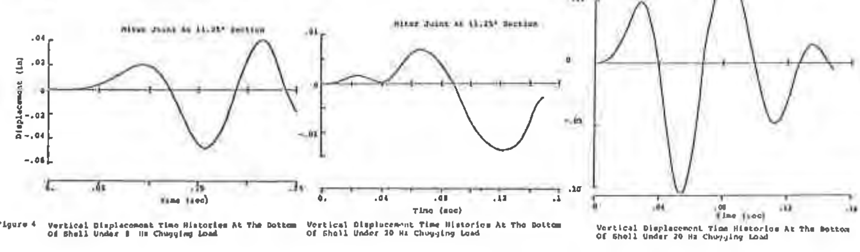

Figure 4 Vertical Displacement Time Histories At The Bottom Of Shell Under 8 Hz Chugging Load

Vertical Displacement Time Histories At The Bottom Of Shell Under 20 Hz Chugging Load

Vertical Displacement Time Histories At The Bottom Of Shell Under 20 Hz Chugging Load

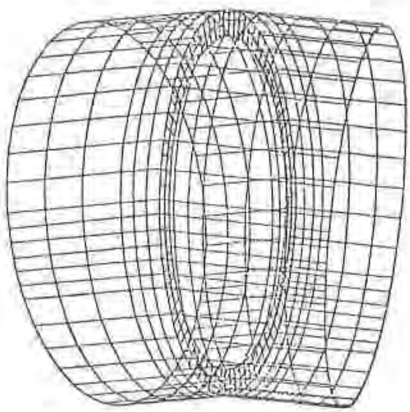

(A) Typical SUPER Element

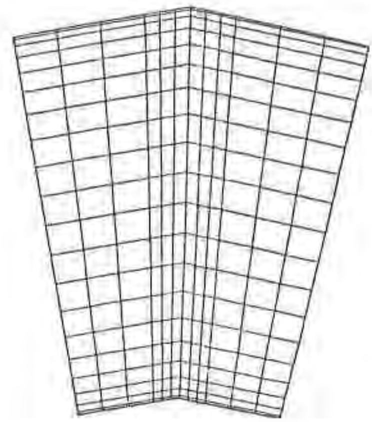

(B) Plane View

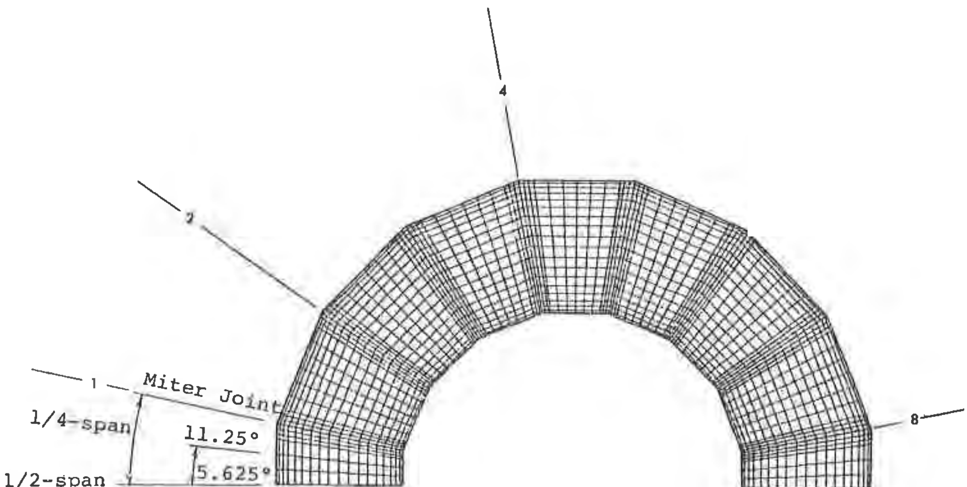

(C) Half Torus Model

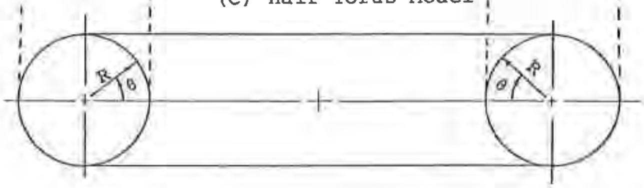

(D) Torus Shell Displacement Coordinate System

Figure **5** Finite Element Model Of Torus